Imbalance Constrained Crossphase Quadratic OPF for Optimal Integration of EV Chargers and PV Inverters in Meshed and Radial Distribution Systems

Araz Bagherzadeh Karimi, *Student Member, IEEE,* Reza Deihimi Kordkandi, *Student Member, IEEE,* Farrokh Aminifar, *Member, IEEE,* Mohsen Hamzeh, *Member, IEEE,*

***Abstract*—Inverter-Based distributed energy resources specially Photovoltaic devices (PVs) and electric vehicle charge stations (EVCS) in the sequel of the power-electronics interface, provide unprecedented flexibility to the system such as the ability to transfer line power across phases. This paper proposes a comprehensive framework for per phase optimal active, reactive, and cross-phase power flow dispatch of PVs and EVCSs. The optimization problem is targeted to maximize the firm benefit of DSO subject to the operational constraints including unbalanced situation tolerability of loads. The problem is formulated as a quadratic objective function with linearized constraints to maintain the tractability with a large number of per phase meshed buses and constraints. A new approximate equation of voltage unbalance factor (VUF) is introduced and used alongside existing linearized equations of other constraints. The applicability of the framework is validated via the unbalanced multi-phase IEEE 33 bus and IEEE 342 bus systems. The results show that the cross-phase dispatch capability significantly helps the system to satisfy the VUF constraint while providing the same maximum profit.**

***Index Terms*—Distributed Energy Resources, Electric Vehicle Charge Stations, Cross-phase power flow, Power Quality, Voltage Imbalance Factor**

NOMENCLATURE

A. General

OF	Objective function

B. Indexes

ℓ	Index of lines
φ, γ	Index of phases
i,j	Index of buses
s	Index of a slack bus

C. Parameters

c_1^s, c_2^s, c_3^s	Cost coefficients of the power provided by the upper voltage system in slack bus *s*
$P_{i_{EV}}^{sch}$	Scheduled consumed active power of an EVCS
$P_{i_{ld}}^{\varphi}, Q_{i_{ld}}^{\varphi}$	Active and reactive powers consumed by load
$P_{i_{PV}}^{sun}$	Maximum available active power of a PV
$R_{ij}^{\varphi\gamma}, X_{ij}^{\varphi\gamma}$	Total resistance and reactance of line from bus *i* to bus *j* and phase φ to phase γ
S_{ij}^{max}	Phase to neutral rated apparent power flow of line from bus *i* to bus *j*
$S_i^{inv}{}_{PV}, S_i^{inv}{}_{EV}$	Phase to neutral rated powers of a PV and EV
V_i	Three-phase Voltage phasor vector
V_i^{min}, V_i^{max}	Minimum and maximum permissible voltage in bus *i*
VUF_i^{min}	Maximum permissible VUF in bus *i*

D. Variables

$P_{i_{EV}}^{\varphi}, Q_{i_{EV}}^{\varphi}$	Active and reactive powers injected from EV
$P_{i_{PV}}^{\varphi}, Q_{i_{PV}}^{\varphi}$	Active and reactive powers injected from PV
$P_{ij}^{\varphi\gamma}, Q_{ij}^{\varphi\gamma}, S_{ij}^{\varphi\gamma}$	Active, reactive and apparent power flows of line from bus *i*, phase φ to bus *j* and phase φ to phase γ
$P_{i\,inject}^{\varphi}, Q_{i\,inject}^{\varphi}$	The injected active and reactive powers
$V_i^{\varphi}, \theta_i^{\varphi}$	Voltage magnitude and angle in bus *i* and phase φ
VUF_i	Voltage imbalance factor in bus number *i*
VUF_i^{apr}	Voltage imbalance factor approximation in bus number *i*

E. Sets

ϕ	Set of phases
L	Set of lines
N	Set of buses
S	Set of Slack Buses

F. Operators

$\hat{A}$	Linear approximation of A
$\{A\}^+, \{A\}^-$	Positive and negative sequence of the three phase phasor vector A

I. INTRODUCTION

MINIMIZING the loss and the operational cost of distribution networks is a critical goal for distribution system operators (DSOs). Distribution networks, by nature, are unbalanced in terms of voltages and currents because of having untransposed lines [1] in distribution feePVs and integration of single-phase generators and loads with highly probabilistic behavior. While voltage imbalance mostly impacts the costumers' power quality, the current imbalance is one of the main causes of loss increase in distribution networks. Mitigation of current and voltage imbalance sources is a serious technical requirement and has drawn the attention of researchers for

many years. We review the approaches revolving around the voltage and current imbalance compensation in the following.

Based on [2] we can decompose the origins of the imbalance into twofold classes: structural and random. The method focusing on the structural aspect includes network reconfiguration [3]–[7] and phase balancing [8]–[10]. These techniques, however, do not have real-time flexibility and continuous controllability for compensating the random component of imbalance. Static transfer system (STS) based methods are proposed to compensate for this [11]. This method may impose switching transients and is less flexible than power electronics devices with continuous controllability. Device-based compensation has been broadly investigated in the literature and proved outstanding capability in mitigating the current imbalance [12]–[15]. These techniques were rarely implemented in the past but their integrations are abruptly on the rise due to the proliferation of Distributed Energy Resources (PVs) and Electrical Vehicle Charge Stations (EVCSs).

Local control strategies for leveraging distributed energy PVs for imbalance compensation have been discussed in [16], [17]. These approaches, as expected, are highly effective but they still lack utilization of full capability of flexible power electronics resources due to the control with incomplete local information status. In the wake of cyber-physical distribution networks enabled by the vast deployment of communication systems, the operational strategies running over the network model with complete system-wide information turn into a real practice [18]–[23]. These methods accommodate the controllability of PV resources and seek to minimize the operation cost in the presence of distribution network imbalance. Voltage imbalance is tackled as a subsidiary objective function in the optimization problem.

Although the active/reactive power generation/absorption of PVs has been fully exploited in reviewed references for the grid management objectives, the capability of EVCSs particularly when used as a dispatchable cross-phase line power transferring device remains unexamined. Also, the minimization of voltage imbalance pursued in some references is not necessarily in line with the least cost operation of the system. To this end, we are envisioning to satisfy the voltage imbalance tolerability of voltage imbalance by putting a soft limit for Voltage Unbalance Factor (VUF) for ensuring the safe operation of customers; motoring devices work out well in real practices. That is, the over mitigation of the system imbalance may be obsolete.

This paper offers a real-time operational strategy based on the single- and three-phase PVs and EVCSs active and reactive powers and cross-phase power transfer adjustment to optimize the operation cost of the distribution system constrained by VUF. Without taking any simplification in the perspective of the optimization model, in the rest of the paper, PVs are assumed to be the prevalent rooftop Photovoltaics (PVs). In order to tackle random imbalance, the optimization problem is established as a real-time optimization problem based on the load, EVCS, and PV data captured by advanced measurement infrastructure (AMI) and the weather condition. In order to support the applicability of the proposed method in real-time management of the PVs and EVCs in large meshed systems, the optimization model is derived in the form of a convex quadratic (QP) problem. To do so, linear power flow equations and line capacity limits are taken into use. The main features of the proposed methodology are:

- Due to tackling the problem in a near real-time scope, random phenomena such as random imbalance, and random PV output fluctuation can be properly compensated.
- PVs and EVCSs resources are concurrently employed in the system and bus level. Their coordination offers further added value in mitigating the imbalance.
- Linearized constraints respect the convexity of the optimization model. The problem is hence tackled more effectively which is a must for real-time applications.
- Other than three-phase power electronics devices, the ever-growing single-phase resources are accommodated as well. This brings additional flexibility for compensating the imbalance which is phase-wise per se.
- Due to the power transferring ability of EVCSs, their active power is also manipulated via cross-phase dispatch alongside the full capability of their reactive power dispatch. This flexibility is of extreme importance since it directly restrains the current imbalance
- Due to not depending on backward-forward or Distflow branch equations [24], the proposed model well fits the heavily meshed and multiple MV connected distribution networks.

The remainder of this paper is organized as follows. Section II formulates the proposed method. The computation implementation is described in III while the results and the corresponding discussion are presented in section IV. Finally, conclusive remarks are presented in Section V.

II. Problem Formulation

The optimization problem is cast based on an OPF model with a single objective function and multiple physical and operational constraints including the imbalance limits. The convex form of the OPF model is employed here and the new constraints are convexified to be in line with the whole model trait.

A. Power Flow model

Three-phase power balance equations consisting of PV injection, EV interaction, and load consumption are expressed as:

$$\forall i \in N, \varphi \in \phi,$$
$$P^{\varphi}_{i_{inject}} + P^{\varphi}_{i_{PV}} = P^{\varphi}_{i_{ld}} + P^{\varphi}_{i_{EV}} + \sum_{j|(i,j)\in L} \sum_{\gamma|\gamma\in\phi} P^{\phi\gamma}_{ij} \quad (1)$$

$$\forall i \in N, \varphi \in \phi,$$
$$Q^{\varphi}_{i_{inject}} + Q^{\varphi}_{i_{PV}} = Q^{\varphi}_{i_{ld}} + Q^{\varphi}_{i_{EV}} + \sum_{j|(i,j)\in L} \sum_{\gamma|\gamma\in\phi} Q^{\phi\gamma}_{ij} \quad (2)$$

It is implicitly assumed in the framework that if a bus does not have a connected device (MV transformer, PV or EVCS)

the corresponding active and reactive power related to that device is forced to be zero. In addition, the self and mutual impedance of all phases are also accounted in the three-phase active and reactive power balance equations. In (1) and (2) the $P_{ij}^{\varphi\gamma}$ and $Q_{ij}^{\varphi\gamma}$ can be written as:

$$\begin{aligned} &\forall(i,j)\in L,\varphi,\gamma\in\phi \\ P_{ij}^{\varphi\gamma} = &\frac{\begin{aligned}R_{ij}^{\varphi\gamma}(V_i^{\varphi})^2 - R_{ij}^{\varphi\gamma}V_i^{\varphi}V_j^{\gamma}\cos(\theta_i^{\varphi}-\theta_j^{\gamma}) \\ +X_{ij}^{\varphi\gamma}V_i^{\varphi}V_j^{\gamma}\sin(\theta_i^{\varphi}-\theta_j^{\gamma})\end{aligned}}{\left(R_{ij}^{\varphi\gamma}\right)^2+\left(X_{ij}^{\varphi\gamma}\right)^2} \end{aligned} \tag{3}$$

$$\begin{aligned} &\forall(i,j)\in L,\varphi,\gamma\in\phi \\ Q_{ij}^{\varphi\gamma} = &\frac{\begin{aligned}X_{ij}^{\varphi\gamma}(V_i^{\varphi})^2 - R_{ij}^{\varphi\gamma}V_i^{\varphi}V_j^{\gamma}\sin(\theta_i^{\varphi}-\theta_j^{\gamma}) \\ +X_{ij}^{\varphi\gamma}V_i^{\varphi}V_j^{\gamma}\cos(\theta_i^{\varphi}-\theta_j^{\gamma})\end{aligned}}{\left(R_{ij}^{\varphi\gamma}\right)^2+\left(X_{ij}^{\varphi\gamma}\right)^2} \end{aligned} \tag{4}$$

In order to have a convex optimization model and tackle the problem via one of the efficient convex solvers, the linearized forms of (1) and (2) for single-phase distribution network are taken from [25] and extended to three-phase unbalanced network. Equations (11) and (12) denote branch active and reactive power losses and are defined based on the linearized power flow expression captured in (5)-(10). As justifiable assumptions in distribution networks, it is assumed that the voltage magnitudes are around 1 p.u. and the angle differences of successive nodes are close to zero.

$$P_{ij}^{\varphi\gamma} \approx P_{ij-1}^{\hat{\varphi}\gamma} + P_{ij-2}^{\hat{\varphi}\gamma} = \hat{P}_{ij}^{\varphi\gamma} \tag{5}$$

$$Q_{ij}^{\varphi\gamma} \approx Q_{ij-1}^{\hat{\varphi}\gamma} + Q_{ij-2}^{\hat{\varphi}\gamma} = \hat{Q}_{ij}^{\varphi\gamma} \tag{6}$$

$$P_{ij-1}^{\hat{\varphi}\gamma} = \frac{r_{ij}^{\varphi\gamma}x_{ij}^{\varphi\gamma}}{r_{ij}^{\varphi\gamma 2}+x_{ij}^{\varphi\gamma 2}}\cdot\frac{V_i^{\varphi}-V_j^{\varphi}}{x_{ij}^{\varphi\gamma}} = k_{ij-1}^{\varphi\gamma}\cdot\frac{V_i^{\varphi}-V_j^{\varphi}}{x_{ij}^{\varphi\gamma}} \tag{7}$$

$$P_{ij-2}^{\hat{\varphi}\gamma} = \frac{x_{ij}^{\varphi\gamma 2}}{r_{ij}^{\varphi\gamma 2}+x_{ij}^{\varphi\gamma 2}}\cdot\frac{\theta_i^{\varphi}-\theta_j^{\varphi}}{x_{ij}^{\varphi\gamma}} = k_{ij-2}^{\varphi\gamma}\cdot\frac{\theta_i^{\varphi}-\theta_j^{\varphi}}{x_{ij}^{\varphi\gamma}} \tag{8}$$

$$Q_{ij-1}^{\hat{\varphi}\gamma} = \frac{-r_{ij}^{\varphi\gamma}x_{ij}^{\varphi\gamma}}{r_{ij}^{\varphi\gamma 2}+x_{ij}^{\varphi\gamma 2}}\cdot\frac{\theta_i^{\varphi}-\theta_j^{\varphi}}{x_{ij}^{\varphi\gamma}} = -k_{ij-1}^{\varphi\gamma}\cdot\frac{\theta_i^{\varphi}-\theta_j^{\varphi}}{x_{ij}^{\varphi\gamma}} \tag{9}$$

$$Q_{ij-2}^{\hat{\varphi}\gamma} = \frac{x_{ij}^{\varphi\gamma 2}}{r_{ij}^{\varphi\gamma 2}+x_{ij}^{\varphi\gamma 2}}\cdot\frac{V_i^{\varphi}-V_j^{\varphi}}{x_{ij}^{\varphi\gamma}} = k_{ij-2}^{\varphi\gamma}\cdot\frac{V_i^{\varphi}-V_j^{\varphi}}{x_{ij}^{\varphi\gamma}} \tag{10}$$

As a result, (1) and (2) can be replaced with (11) and (12):

$$\begin{aligned} P_{i_{inject}}^{\varphi} + P_{i_{PV}}^{\varphi} = P_{i_{ld}}^{\varphi} + P_{i_{EV}}^{\varphi} \\ + \sum_{\ell|(i,j)\in L}\sum_{\gamma|\gamma\in\phi} P_{ij}^{\hat{\varphi}\gamma} \end{aligned} \tag{11}$$

$$\begin{aligned} Q_{i_{inject}}^{\varphi} + Q_{i_{PV}}^{\varphi} = Q_{i_{ld}}^{\varphi} + Q_{i_{EV}}^{\varphi} \\ + \sum_{\ell|(i,j)\in L}\sum_{\gamma|\gamma\in\phi} Q_{ij}^{\hat{\varphi}\gamma} \end{aligned} \tag{12}$$

B. Capacity constraint

Capacity of distribution lines should guarantee the secure operation of the system. So, it can be written as:

$$\begin{aligned} &\forall(i,j)\in\ell,\forall\varphi,\varphi\in\phi \\ &S_{ij}^{\varphi\varphi} = \sqrt{P_{ij}^{\varphi\varphi 2}+Q_{ij}^{\varphi\varphi 2}} \le S_{ij}^{max} \end{aligned} \tag{13}$$

In perspective of optimization problem parameters and variables, the equation (13) is nonlinear and nonconvex. Therefore, linear approximation using piecewise linearization method [26] is applied to maintain the linear and convex form of the problem and can be shown as:

$$\begin{aligned} &\forall h,h\in N,h\le H,\forall(i,j)\in\ell,\forall\varphi,\varphi\in\phi \\ &\left(\sin\left(\frac{360^{\circ}h}{H}\right)-\sin\left(\frac{360^{\circ}}{H}(h-1)\right)\right)P_{ij}^{\varphi\varphi}- \\ &\left(\cos\left(\frac{360^{\circ}h}{H}\right)-\cos\left(\frac{360^{\circ}}{H}(h-1)\right)\right)Q_{ij}^{\varphi\varphi} \\ &\le S_{ij}^{max}\times\sin\left(\frac{360^{\circ}}{H}\right) \end{aligned} \tag{14}$$

C. Voltage constraints: magnitude, imbalance factor

The hard margin constraint voltage magnitude constraint is implemented as:

$$\forall i,\varphi,\ i\in N,\varphi\in\phi,\quad V_{min}\le V_i^{\varphi}\le V_{max} \tag{15}$$

In (15) the V_{min} and V_{max} are the voltage magnitude limits determined by the standards. In order to maintain power quality standards in unbalanced system the VUF standard is taken into consideration [27]. Equation (16) demonstrates the definition of VUF.

$$VUF_i = \frac{|V_i^-|}{|V_i^+|} \le VUF_{max} \tag{16}$$

It is assumed that the VUF can be approximated by a quadratic function:

$$\begin{aligned} VUF_i \approx VUF_i^{apr} = \alpha_i((V_i^a-V_i^b)^2+(V_i^b-V_i^c)^2 \\ +(V_i^c-V_i^a)^2)+\beta_i(((\theta_i^a-0)-(\theta_i^b-\frac{2\pi}{3}))^2+((\theta_i^c-\frac{4\pi}{3}) \\ -(\theta_i^a-0))^2+((\theta_i^b-\frac{2\pi}{3})-(\theta_i^c-\frac{4\pi}{3}))^2) \end{aligned} \tag{17}$$

$$\begin{aligned} VUF_i^{apr} = \sum_{0<m<22}\sum_{\varphi,\gamma\in\phi}\alpha_i(V_i^{\varphi})^m(V_i^{\gamma})^1-m+(V_i^{\varphi})^m(\theta_i^{\gamma})^1-m \\ +(\theta_i^{\varphi})^m(\theta_i^{\gamma})^1-m \end{aligned} \tag{18}$$

In (18) the θ_i^{φ} are mapped to origin, and α_i, β_i are the soft margin VUF minimizer coefficients. The ratio of α_i and β_i can be determined by performing a regression in a set of data points in the nominal voltage magnitude and angle range. However, the values of α_i and β_i are used to quantify the

trade-off in the epsilon constraint method discussed in the next subsection. This flexibility in the value will enable prioritizing this power quality constrain in certain buses. In other words, improve imbalance of a certain bus by only exploiting the existing system flexibility in the operation, without performing local modifications or installations.

D. Objective function

Without loss of generality, the minimum operational cost of the system is sought here as (19).

$$\begin{aligned} &OF \in R, \\ &OF = \sum_{s \in S} c_1^s + c_2^s P_{inject_s^\varphi} + c_3^s (P_{inject_s^\varphi})^2 \end{aligned} \tag{19}$$

The active power injection of PVs and reactive power support of EVCSs are assumed to be costless. The objective functions can be readily tailored for meshed and multiple input distribution networks connected to MV systems with different cost terms. The objective function can also imply either minimization of the cost or maximization of firm benefit in the highly PV penetrated, and reverse power flow enabled systems. It is quite straightforward to replace it with maximum social welfare, maximum firm benefit, etc., or even proceed with multiple objectives, for the purpose of this paper the multi objective objective function is presented as (20).

$$\begin{aligned} &OF \in R, \\ &OF = \sum_{s \in S} c_1^s + c_2^s P_{inject_s^\varphi} + c_3^s (P_{inject_s^\varphi})^2 + \sum_{i \in N} VUF_i^{apr} \end{aligned} \tag{20}$$

In order to quantify the trade-off, the epsilon constraint method can be implemented by sweeping the values of the weighted penalty factor implementation of VUF_i^{apr}.

E. EVCS models

EVCSs are considered both single- and three-phase in distribution systems. While they can flexibly provide reactive power based on system optimization, their consumed active power is assumed to be constant and adjusted based on the customer charging preference and the battery and inverter capability in a certain period of time. Nevertheless, they can provide some flexibility over consumed active power in each time interval thanks to their schedulability. Because we are targeted to perform the optimization in the near real time scope to handle random phenomena, we prefer to ignore this capability at least in the scope of this study. The formulation of a single-phase EVCS in phase κ is shown in (21)-(23). For simplification, EVCSs are shortened to EVs in the optimization formulations.

$$\forall i, i \in N \quad P_{i_{EV}}^{\kappa} = P_{i_{EV}}^{sch} \tag{21}$$

$$\forall i, i \in N \;\; \forall \varphi, \varphi \in \phi |\, \varphi \neq \kappa, \quad P_i^{EV} = 0 \tag{22}$$

$$\begin{aligned} \forall i, i \in N \quad -\sqrt{(S_{i_{EV}}^{inv})^2 - (P_{i_{EV}}^{\kappa})^2} \leq Q_{i_{EV}}^{\kappa} \\ \leq +\sqrt{(S_{i_{EV}}^{inv})^2 - (P_{i_{EV}}^{\kappa})^2} \end{aligned} \tag{23}$$

The variable $Q_{i_{EV}}^{\kappa}$ can be derived based on the result of the optimization problem. Equations (24)-(26) show the three-phase EVCS model and corresponding linearization. In the three-phase case, (21) and (22) are changed to (24) in which the cross-phase active power transfer is also enabled.

$$\forall i \in N, \sum_{\varphi \in \phi} P_{i_{EV}}^{\varphi} = P_{i_{EV}}^{sch} \tag{24}$$

$$\forall i, i \in N, \forall \varphi, \varphi \in \phi, \quad \sqrt{(P_{i_{EV}}^{\varphi})^2 + (Q_{i_{EV}}^{\varphi})^2} \leq S_{i_{EV}}^{inv} \tag{25}$$

$$\begin{aligned} &\forall h, h \in H, \forall i, i \in N, \forall \varphi, \varphi \in \phi \\ &\left(\sin\left(\frac{360^\circ h}{H}\right) - \sin\left(\frac{360^\circ}{H}(h-1)\right)\right) P_{i_{EV}}^{\varphi} \\ &- \left(\cos\left(\frac{360^\circ h}{H}\right) - \cos\left(\frac{360^\circ}{H}(h-1)\right)\right) Q_{i_{EV}}^{\varphi} \\ &\leq S_{i_{EV}}^{inv} \times \sin\left(\frac{360^\circ}{H}\right) \end{aligned} \tag{26}$$

Therefore, corresponding $P_{i_{EV}}^{\varphi}$(cross-phase active power) can be derived based on the optimization results as well as the $Q_{i_{EV}}^{\varphi}$. The noteworthy point is that even during the off hours of EVCSs, the active power can be transferred between phases like an active power line conditioner [14]. This enables the EVCSs to provide more active ancillary services if needed and make them more economically reasonable.

F. PVs model

As same as the EVCSs, PVs are installed as three-phase and single-phase in distribution networks. While the three-phase PVs can contribute to the balancing and voltage magnitude control, the single-phase configurations may be harmful to the system power quality when used uncontrolled. Therefore, PV management not only can help the optimization problem to have enough flexibility to satisfy its objective, but also it is necessary for maintaining the power quality standards. The single-phase PV in phase κ can be modeled as:

$$\forall i, i \in N, \; 0 \leq P_{i_{PV}}^{\kappa} \leq P_{i_{PV}}^{sun} \tag{27}$$

$$\forall i, i \in N, \; \forall \varphi, \varphi \in \phi | \varphi \neq \kappa, \; P_{i_{PV}}^{\varphi} = 0 \tag{28}$$

$$\forall i, i \in N, \;\; \sqrt{\left(P_{i_{PV}}^{\kappa}\right)^2 + \left(Q_{i_{PV}}^{\kappa}\right)^2} \leq S_{i_{PV}}^{inv} \tag{29}$$

With the linear approximation, (29) can be replaced by:

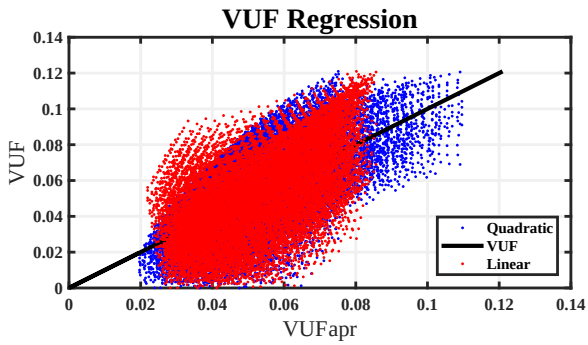

Fig. 1. Scatter Plot of Linear and Quadratic Regression of VUF

$$\forall h, h \in H, \forall i, i \in N,$$
$$\left(\sin\left(\frac{360^\circ h}{H}\right) - \sin\left(\frac{360^\circ}{H}(h-1)\right)\right) P^{\kappa}_{i_{PV}}$$
$$-\left(\cos\left(\frac{360^\circ h}{H}\right) - \cos\left(\frac{360^\circ}{H}(h-1)\right)\right) Q^{\kappa}_{i_{PV}} \quad (30)$$
$$\leq S^{inv}_{i_{PV}} \times \sin\left(\frac{360^\circ}{H}\right)$$

The corresponding $P^{\kappa}_{i_{PV}}$ and $P^{\kappa}_{i_{PV}}$ are derived as a result of the optimization problem. The three-phase PV model and the approximation are presented in (31),(32), and (33), respectively:

$$\forall i \in N,\ 0 \leq \sum_{\varphi \in \phi} P^{\varphi}_{i_{PV}} \leq P^{sun}_{i_{PV}} \quad (31)$$

$$\forall i, i \in N, \forall \varphi, \varphi \in \phi, \quad \sqrt{(P^{\varphi}_{i_{PV}})^2 + (Q^{\varphi}_{i_{PV}})^2} \leq S^{inv}_{i_{PV}} \quad (32)$$

$$\forall h, h \in H, \forall i, i \in N, \forall \varphi, \varphi \in \phi$$
$$\left(\sin\left(\frac{360^\circ h}{H}\right) - \sin\left(\frac{360^\circ}{H}(h-1)\right)\right) P^{\varphi}_{i_{PV}}$$
$$-\left(\cos\left(\frac{360^\circ h}{H}\right) - \cos\left(\frac{360^\circ}{H}(h-1)\right)\right) Q^{\varphi}_{i_{PV}} \quad (33)$$
$$\leq S^{inv}_{i_{PV}} \times \sin\left(\frac{360^\circ}{H}\right)$$

Finally, the $P^{\varphi}_{i_{PV}}$ and $Q^{\varphi}_{i_{PV}}$ can be derived as a result of the optimization problem. To sum up, the QP framework will be the minimization of the objective function of (19) subject to (11), (12), (14), (23)-(27), (29)-(31), (33), (34) and (36).

III. VUF Approximation and Pareto Front

A. VUF Quadratic SVM Regression

B. Pareto front trade-off

IV. Computational Implementation

A. Input Structure and Test Cases

The input Data structure is built and developed based on the MATPOWER structure [28]. The Matpower test case structure is modified from single line balanced to three phase unbalanced in order to be able to add the three-phase unbalanced

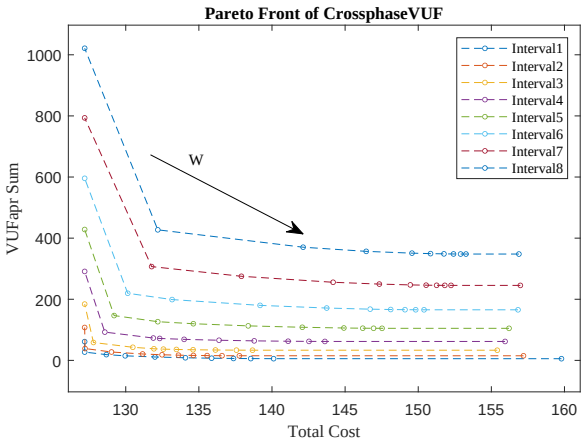

Fig. 2. Pareto front of *Crossphase VUF* method in *PVEVafternoon* scenario

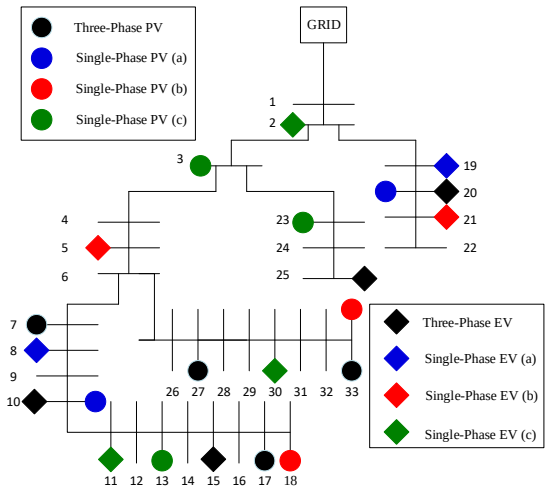

Fig. 3. IEEE 33-bus system

test cases to the case library. For the purpose of this paper, two unbalanced standard systems are added to Matpower library; IEEE 33 Bus [24] and the 192 LV buses of the IEEE 342-bus test system [29]. The two systems are chosen in such away that cover different voltage levels, bus numbers, topology type (meshed or radial) and number of slack buses. Assuming the symmetrical configuration of its lines and cables, the IEEE 33-bus system is modified to be balanced three-phase system and then the loads are forced to be unbalanced by load intensity factor which will be defined later in the paper. However, the 192 LV buses of the IEEE 342-bus test system is inherently unbalanced and heavily meshed and connected to the MV system from different nodes in order to maintain reliability and satisfy the high load density. For the purpose of this research, single-phase and three phase PV and EVCs with different penetration levels are added to the test cases. Fig. 3 and 4 demonstrate the PV and EV locations of the mentioned systems respectively. It worth to mention that the location of EVs and PVs are occasionally overlapped to create a more intense test environment for the proposed method. The details of the test systems are elaborated in table I.

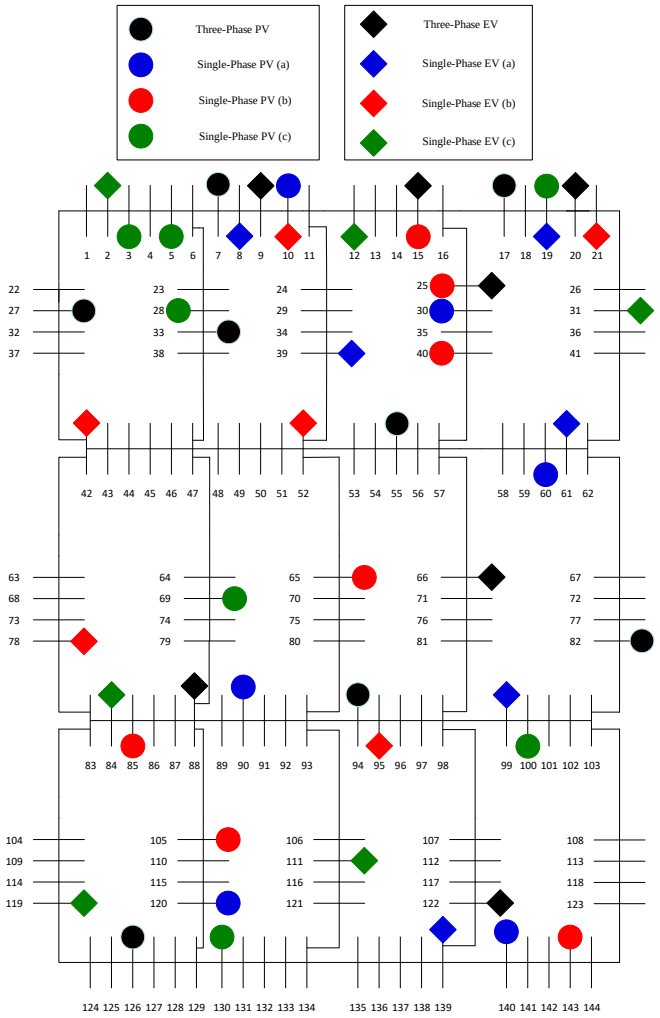

Fig. 4. IEEE 192-bus system

TABLE I
SYSTEM PARAMETERS IN THE FIRST TIME INTERVAL

System	33-Bus	192-Bus
L-n Voltage	12.6kv	120
Min Voltage	0.9 p.u	0.9 p.u
Max Voltage	1.1 p.u	1.1 p.u
Cost Coefficient c_1	3	3
Cost Coefficient c_2	0.1	0.1
Cost Coefficient c_3	0	0
Base MVA	100MVA	100MVA
Sum of Loads	3.75MW	2.9MW
Average of Loads	0.11MW	0.02MW
Sum of Reactive Loads	2.3MW	1.82MW
Average of Reactive Loads	0.07MVAR	0.012MVAR
Three-phase EV Charger Capacity	0.54MVA	0.54MVA
Single-phase EV Active Power Consumption	0.18MVA	0.03MVA
Three-phase EV Active Power Consumption	0.54MVA	0.09MVA
Single-Phase PV Active Power Generation	0.06MVA	0.03MVA
Three-phase PV Ative Power Generation	0.4MVA	0.1MVA
Three-phase PV Capacity	0.9MVA	0.9MVA
Slack Bus Locations	1	144-192

TABLE II
SUB-METHODS USED FOR ABLATION STUDY

Sub-Method	Solver	Equations
Fixed	Matpower	(1-4), (13), (15), (19), (21), (23), (27), (29)
OPF	CVX	(5-12), (14-15), (19), (21), (23), (27), (30)
OPF VUF	CVX	(5-12), (14-15), (18), (20-21), (23), (27), (30)
Crossphase	CVX	(5-12), (14-15), (19), (21-22), (23-24), (26-28), (30-31), (33)
Crossphase VUF	CVX	(5-12), (14-15), (18), (20-22), (23-24), (26-28), (30-31), (33)

B. Method Clustering

The proposed method is clustered into Five sub-methods presented in table II to form an ablation study. The *Fixed* method is regular OPF solver in Matpower extended to three phase systems. Consequently, three-phase EVs and PVs are considered as three single-phase models. The *OPF* method is the linearized form of the *Fixed* method solved in CVX. The *OPF VUF* method is the *OPF* method that consideres the VUF constraint. Similarly, the *Crossphase* method is the *OPF* with enabling the crossphase capability of PVs and EVs. Finally the *CrossPhase VUF* method integrates all the contributions of this paper in one method. Both Matpower and CVX solvers are run in the the MATLAB 2022a, Intel Core i5 8250U (1.6-1.8 GHz) CPU, and 8 GB DDR3-1333 (667 MHz) memory Environment.

C. Operation Scenarios and time intervals

In order to test the individual and combined contribution of the each inverter type, three scenarios are considered as *Base(NC)*, *PV-noon(NC)*, *Ev-night(NC)*, and *PV-EV-Afternoon*. In addition, due to the fact that, unlike the *Fixed*, *OPF* and *OPF-VUF* methods, *Crossphase* and *Crossphase OPF* methods have the ability to exploit the active power capacity of the inverters in their non operation hours, three more scenarios are added as *Base(C)*, *PV-noon(C)*, *Ev-night(C)*, to evalate the contribution of each inverter type in non operational hours. The Table III demonstrates connectivity status of the inverters in each of these scenarios.

All of the scenarios consists of eighth time intervals each having a different load imbalance level as shown in figure

TABLE III
SCENARIOS CONSIDERED FOR SIMULATION

Scenarios	Three- and Single-phase EV Inverters	Three- and Single-phase PV Inverters
Base(NC)	Inactive	Inactive
Base(C)	Active for Crossphase	Active for Crossphase
PV-Noon(NC)	Inactive	Normal Operation
PV-Noon(C)	Active for Crossphase	Normal Operation
EV-Night(NC)	Normal Operation	Inactive
EV-Night(C)	Normal Operation	Active for Crossphase
PV-EV-Afternoon	Normal Operation	Normal Operation

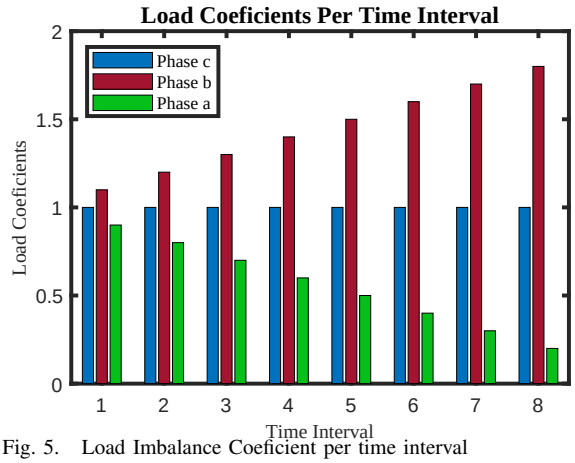

Fig. 5. Load Imbalance Coeficient per time interval

5. The load imbalance (Active and Reactive) is getting worse linearly in each interval while maintaining a constant total load consumption in order to obtain standardized load flow results.

V. Results and Discussion

In this section, the effectiveness of the proposed method in minimizing power loss and total cost, reducing the VUF violated buses, and ability to relieve capacity of the test system is presented and discussed. First, the sub-methods of table II are compared in terms of the aforementioned output properties in the worst case load imbalance scenario (time interval 8). Then output properties are presented for the *CrossPhase VUF* method in all load imbalance intensities and operation scenarios.

A. Total power loss of the test systems

Total power loss of the test systems are pointed out in Tables. IV and V. In the studied scenarios, eight-time intervals with the incremental rate in voltage imbalance is considered. Therefore, voltage imbalance is the highest amount in interval eight. Analyzing Table.IV clears that by increasing VUF, total power loss of the IEEE 33-Bus system experiences an upward trend. Also, the proposed method of this paper has the lowest power loss amounts compared to the other common methods. Moreover, implementing VUF constraints into the objective function of the cross-phase dispatching method has a positive effect in reducing the loss of the 33-Bus system. On the other hand, Table. V depicts the total loss in the IEEE 192-Bus system. Assessing the obtained results demonstrates that cross phase approach wastes power less than the common OPF method. Nevertheless, adding VUF constraints to the mentioned methods increases the loss of the system partially.

In addition, superiority of the corresponding scenarios in which the power electronic inverters contribute for power displacing among the phases (scenarios ending with "C") over non-contributing ones (scenarios ending with "NC") are shown in Tables. VI and VII for IEEE 33-Bus and IEEE 342-Bus systems, respectively. The results clearly show that the contribution of the inverters diminishes the total power loss at most of the times. However, in the case of IEEE 342-Bus system only in the "PV-Noon" scenario a reduction in power loss of the system occurs.

TABLE IV
Total power loss in IEEE 33-Bus system with different dispatching methods (kW)

Hour	Fixed	OPF	OPF-VUF	Crossphase	Crossphase-VUF
1	4.88	4.87	4.68	4.86	5.01
2	4.98	4.97	4.81	4.92	5.05
3	5.15	5.14	5.13	5.06	5.16
4	5.39	5.37	5.35	5.26	5.32
5	5.70	5.69	5.60	5.54	5.56
6	6.08	6.07	5.91	5.88	5.86
7	6.53	6.52	6.29	6.29	6.22
8	7.06	7.04	6.75	6.78	6.66

TABLE V
Total power loss in IEEE 192-Bus system with different dispatching methods (kW)

Hour	Fixed	OPF	OPF-VUF	Crossphase	Crossphase-VUF
1	14.15	14.40	15.51	14.42	14.80
2	14.47	14.72	16.11	14.72	14.82
3	15.00	15.25	16.62	15.24	15.14
4	15.74	16.00	17.16	15.95	15.99
5	16.70	16.94	17.85	16.86	17.29
6	17.87	18.07	18.72	17.92	18.53
7	19.25	19.43	19.81	19.29	19.79
8	20.85	21.00	21.09	20.81	20.97

B. Total cost of the studied systems

Total cost of the systems is evaluated using the presented strategy and the other common methods in Tables.VIII and IX. Assessing Tables.VIII and IX proves that using a cross-phase approach reduces the total cost of the systems. As it is visible, utilizing the other conventional methods is not so profitable compared to the novel strategy of this paper. Adding VUF constraints to the objective function increases the total cost, however that is the charge DNOs should pay to minimize the voltage imbalance factor of the system. On the other hand, the extra cost of the cross-phase approach considering the VUF constraint is still lower than the other common strategy with VUF constraint (Table. IX).

TABLE VI
Total power loss of the 33-Bus system with crossphase-VUF method in different scenarios (kW)

Hour	1	2	3	4	5	6	7	8
Base(C)	5.35	5.34	5.42	5.20	5.75	5.75	6.10	6.51
Base (NC)	5.31	5.41	5.59	5.83	6.15	6.53	6.99	7.51
EV-Night (C)	5.48	5.38	5.52	5.62	5.84	6.12	6.48	6.86
EV-Night (NC)	5.41	5.50	5.66	5.88	6.17	6.54	6.97	7.47
PV-Noon (C)	4.77	4.94	5.06	5.25	5.50	5.79	6.16	6.60
PV-Noon (NC)	4.81	4.92	5.09	5.27	5.52	5.84	6.23	6.70

TABLE VII
TOTAL POWER LOSS OF THE 342-BUS SYSTEM WITH CROSSPHASE-VUF METHOD IN DIFFERENT SCENARIOS (KW)

Hour	1	2	3	4	5	6	7	8
Base(C)	16.72	16.85	17.17	17.79	18.53	19.35	20.31	21.38
Base (NC)	16.48	16.79	17.32	18.06	19.00	20.16	21.53	23.11
EV-Night (C)	19.85	20.02	20.38	21.01	21.77	22.64	23.57	24.69
EV-Night (NC)	19.60	19.77	20.17	20.79	21.59	22.58	23.77	25.18
PV-Noon (C)	12.52	12.70	12.98	13.64	14.93	16.12	17.30	18.46
PV-Noon (NC)	12.68	12.87	13.32	14.24	15.68	16.97	18.40	19.77

TABLE VIII
TOTAL COST OF THE IEEE 33-BUS SYSTEM DURING " PV-EV-AFTERNOON" SCENARIO WITH DIFFERENT METHODS

Hour	**Fixed**	**OPF**	**OPF-VUF**	**Crossphase**	**Crossphase-VUF**
1	326.31	326.31	326.31	325.54	325.54
2	328.88	328.88	331.81	327.06	327.06
3	333.11	333.11	336.93	330.25	332.25
4	333.99	338.99	344.55	335.09	338.09
5	346.54	346.54	351.72	341.29	344.55
6	355.73	355.73	360.53	349.75	354.44
7	366.59	366.59	377.01	359.56	364.86
8	379.10	379.10	385.60	371.03	375.92

As well as results of the power loss, the total cost of the studied-systems are less in the scenarios with inverter contribution compared to their counterparts without inverter contribution (Tables. X and XI). Also, it should be mentioned that the total cost of the IEEE 342-Bus system only gets better in the "PV-Noon" scenario, however the total costs of the other scenarios with and without inverter contribution are the same in the IEEE 342-Bus system (Table. XI).

C. Voltage imbalance in the studied systems

This subsection aims to evaluate the voltage imbalance factor of the test systems during the worst-case scenario (eighth time interval) using the conventional and proposed dispatching frameworks statistically. For this purpose, Tables. XII and XIII demonstrate the percentage of the buses in each system, which exceeded the determined amount in IEEE 1159. As it is visible, while using the proposed crossphase-VUF strategy, the percentage rate of imbalance factor is the lowest in both of the test systems during the worst-case scenario.

TABLE IX
TOTAL COST OF THE IEEE 342-BUS SYSTEM DURING " PV-EV-AFTERNOON" SCENARIO WITH DIFFERENT METHODS

Hour	**Fixed**	**OPF**	**OPF-VUF**	**Crossphase**	**Crossphase-VUF**
1	127.19	127.19	140.14	127.19	134.06
2	127.19	127.19	144.80	127.19	133.60
3	127.19	127.19	146.86	127.19	133.46
4	127.19	127.19	147.20	127.19	136.37
5	127.19	127.19	147.22	127.19	142.07
6	127.19	127.19	147.23	127.19	146.71
7	127.19	127.19	147.20	127.19	149.45
8	127.19	127.19	147.19	127.19	150.84

TABLE X
TOTAL COST OF THE IEEE 33-BUS SYSTEM DURING DIFFERENT SCENARIOS WITH CROSS-PHASE-VUF METHOD

Hour	1	2	3	4	5	6	7	8
Base(C)	347.16	348.27	351.06	355.77	361.87	369.01	375.65	381.87
Base (NC)	347.94	350.42	354.56	360.36	367.81	367.92	387.69	400.11
EV-Night (C)	355.24	355.99	358.14	363.74	369.94	377.86	387.47	401.58
EV-Night (NC)	355.59	357.56	361.19	366.46	373.40	381.99	392.24	404.14
PV-Noon (C)	317.78	319.13	324.36	330.45	337.35	346.94	357.41	369.02
PV-Noon (NC)	318.07	320.13	326.48	332.13	339.27	349.42	360.33	374.39

TABLE XI
TOTAL COST OF THE IEEE 342-BUS SYSTEM DURING DIFFERENT SCENARIOS WITH CROSS-PHASE-VUF METHOD

Hour	1	2	3	4	5	6	7	8
Base(C)	155.19	155.19	155.19	155.19	155.19	155.19	155.19	155.19
Base (NC)	155.19	155.19	155.19	155.19	155.19	155.19	155.19	155.19
EV-Night (C)	171.19	171.19	171.19	171.19	171.19	171.19	171.19	171.19
EV-Night (NC)	171.19	171.19	171.19	171.19	171.19	171.19	171.19	171.19
PV-Noon (C)	118.97	118.92	119.31	121.10	126.94	131.45	134.58	136.64
PV-Noon (NC)	121.15	120.70	120.90	123.32	129.92	134.27	138.13	140.28

Therefore, it can be concluded that this method performs better than the other dispatching solutions.

Furthermore, the effect of the contributing inverters in reducing imbalance factor is reported in Tables. XIV and XV. Analyzing these tables proves that in the scenarios in which inverters contribute to displace power from one phase to another, the percentage of buses violating the 2% limit is a very small amount.

D. Free capacity of the studied systems

Also, relieving the lines capacity is one of the goals of the presented method in this paper. Eq.(34) shows the calculation process of this amount, in which APM stands for apparent power mismatch.

TABLE XII
PERCENTAGE OF THE BUSES OF IEEE 33-BUS SYSTEM VIOLATING THE IEEE 1159 STANDARD VIA VARIOUS DISPATCHING METHODS ($\%$)

Fixed	**OPF**	**OPF-VUF**	**Crossphase**	**Crossphase-VUF**
48.5	48.5	39.4	45.5	30.3

TABLE XIII
PERCENTAGE OF THE BUSES OF IEEE 342-BUS SYSTEM VIOLATING THE IEEE 1159 STANDARD VIA VARIOUS DISPATCHING METHODS ($\%$)

Fixed	**OPF**	**OPF-VUF**	**Crossphase**	**Crossphase-VUF**
34.89	33.85	9.89	31.25	2.60

TABLE XIV
PERCENTAGE OF THE BUSES IEEE 33-BUS SYSTEM VIOLATING THE IEEE 1159 STANDARD DURING DIFFERENT SCENARIOS (%)

Base (NC)	Base (C)	PV-Noon (NC)	PV-Noon (C)	EV-Night (NC)	EV-Night (C)
74.20	42.70	46.30	40.70	71.10	44.30

TABLE XV
PERCENTAGE OF THE BUSES IEEE 342-BUS SYSTEM VIOLATING THE IEEE 1159 STANDARD DURING DIFFERENT SCENARIOS (%)

Base (NC)	Base (C)	PV-Noon (NC)	PV-Noon (C)	EV-Night (NC)	EV-Night (C)
33.80	2.00	3.60	1.60	18.20	3.10

$$\sum_{(i,j)=1-l} (S_{ij} - APM_{ij}) \tag{34}$$

Comparing the derived amounts in Tables. XVI and XVII declares that utilizing the Crossphase-VUF method maximizes the total empty capacity of the test systems. Moreover, the positive impact of power displacing through phases is visible in different scenarios reported in Tables. XVIII and XIX.

VI. CONCLUSION

As the same as the EVCSs, PVs are installed as three-phase and single-phase in distribution networks. While the three-phase PVs can contribute to the balancing and voltage magnitude control, the single-phase configurations may be harmful to the system power quality when used uncontrolled. Therefore, PV management not only can help the optimization problem to have enough flexibility to satisfy its objective, but also it is necessary for maintaining the power quality standards. The VCs also will be a prevalent source in near future and in both single- and three-phase forms they have the ability of reactive power injection and in their three-phase form they have the additional ability of cross-phase active power transfer.

A framework based on concurrent optimal operation of PVs and EVCSs is presented and tested in this paper which is able to handle the voltage imbalance and optimize the distribution system in a real-time manner with great flexibility thanks to the several reactive power injections, manageable active power injections, and cross-phase active power transfer options. Thanks to the use of several novels and existing linearization methods the framework is able to be implemented in near real-time. In addition, because of the 1) several flexibilities provided by PVs and EVCSs and 2) holding the VUF unPV the designated limit instead of forcing it to be zero, the objective function is not significantly compromised by the constraints.

As a direct benefit of the proposed method in the market studies, Based on the results, a new LMP-VUF which is the difference of the cross-phase and cross-phase VUF total costs can be introduced which can be used to modify power cost for each customer in the market perspective.

TABLE XVI
THE AMOUNT OF MCR WHILE USING DIFFERENT METHODS IN IEEE 33-BUS SYSTEM (KVA)

Fixed	OPF	OPF-VUF	Crossphase	Crossphase-VUF
186.13	186.26	188.59	187.88	189.33

TABLE XVII
THE AMOUNT OF MCR WHILE USING DIFFERENT METHODS IN IEEE 342-BUS SYSTEM (KVA)

Fixed	OPF	OPF-VUF	Crossphase	Crossphase-VUF
19.20	19.19	19.52	19.24	19.76

TABLE XVIII
THE MCR AMOUNT OF THE IEEE 33-BUS SYSTEM IN DIFFERENT SCENARIOS (KVA)

Base (NC)	Base (C)	PV-Noon (NC)	PV-Noon (C)	EV-Night (NC)	EV-Night (C)
184.20	189.72	188.38	189.41	185.16	188.22

TABLE XIX
THE MCR AMOUNT OF THE IEEE 342-BUS SYSTEM IN DIFFERENT SCENARIOS (KVA)

Base (NC)	Base (C)	PV-Noon (NC)	PV-Noon (C)	EV-Night (NC)	EV-Night (C)
18.42	19.33	19.38	19.95	18.34	18.62

REFERENCES

[1] P. Paranavithana, S. Perera, R. Koch, and Z. Emin, "Global voltage unbalance in mv networks due to line asymmetries," *IEEE transactions on power delivery*, vol. 24, no. 4, pp. 2353–2360, 2009.

[2] W. Kong, K. Ma, and Q. Wu, "Three-phase power imbalance decomposition into systematic imbalance and random imbalance," *IEEE Transactions on Power Systems*, vol. 33, no. 3, pp. 3001–3012, 2017.

[3] V. Borozan, D. Rajicic, and R. Ackovski, "Minimum loss reconfiguration of unbalanced distribution networks," *IEEE Transactions on Power Delivery*, vol. 12, no. 1, pp. 435–442, 1997.

[4] A. B. Morton and I. M. Mareels, "An efficient brute-force solution to the network reconfiguration problem," *IEEE Transactions on Power Delivery*, vol. 15, no. 3, pp. 996–1000, 2000.

[5] E. Dall'Anese and G. B. Giannakis, "Sparsity-leveraging reconfiguration of smart distribution systems," *IEEE transactions on power delivery*, vol. 29, no. 3, pp. 1417–1426, 2014.

[6] F. Ding and K. A. Loparo, "Feeder reconfiguration for unbalanced distribution systems with distributed generation: A hierarchical decentralized approach," *IEEE Transactions on Power Systems*, vol. 31, no. 2, pp. 1633–1642, 2015.

[7] Y.-Y. Fu and H.-D. Chiang, "Toward optimal multiperiod network reconfiguration for increasing the hosting capacity of distribution networks," *IEEE Transactions on Power Delivery*, vol. 33, no. 5, pp. 2294–2304, 2018.

[8] J. Zhu, M.-Y. Chow, and F. Zhang, "Phase balancing using mixed-integer programming [distribution feeders]," *IEEE transactions on power systems*, vol. 13, no. 4, pp. 1487–1492, 1998.

[9] T.-H. Chen and J.-T. Cherng, "Optimal phase arrangement of distribution transformers connected to a primary feeder for system unbalance improvement and loss reduction using a genetic algorithm," in *Proceedings of the 21st International Conference on Power Industry Computer Applications. Connecting Utilities. PICA 99. To the Millennium and Beyond (Cat. No. 99CH36351)*. IEEE, 1999, pp. 145–151.

[10] M. W. Siti, D. V. Nicolae, A. A. Jimoh, and A. Ukil, "Reconfiguration and load balancing in the lv and mv distribution networks for optimal performance," *IEEE transactions on power delivery*, vol. 22, no. 4, pp. 2534–2540, 2007.

[11] F. Ding and M. J. Mousavi, "On per-phase topology control and switching in emerging distribution systems," *IEEE Transactions on Power Delivery*, vol. 33, no. 5, pp. 2373–2383, 2018.
[12] G. E. Valderrama, P. Mattavelli, and A. M. Stankovic, "Reactive power and imbalance compensation using statcom with dissipativity-based control," *IEEE Transactions on Control Systems Technology*, vol. 9, no. 5, pp. 718–727, 2001.
[13] R. C. Pires, "Unbalanced phase-to-phase voltage compensators applied to radial distribution feeders," *IEEE transactions on power delivery*, vol. 19, no. 2, pp. 806–812, 2004.
[14] P. Salmerón, J. Montano, J. Vázquez, J. Prieto, and A. Pérez, "Compensation in nonsinusoidal, unbalanced three-phase four-wire systems with active power-line conditioner," *IEEE transactions on power delivery*, vol. 19, no. 4, pp. 1968–1974, 2004.
[15] Y. Xu, J. D. Kueck, L. M. Tolbert, and D. T. Rizy, "Voltage and current unbalance compensation using a parallel active filter," in *2007 IEEE Power Electronics Specialists Conference*. IEEE, 2007, pp. 2919–2925.
[16] M. Singh, V. Khadkikar, A. Chandra, and R. K. Varma, "Grid interconnection of renewable energy sources at the distribution level with power-quality improvement features," *IEEE transactions on power delivery*, vol. 26, no. 1, pp. 307–315, 2010.
[17] S. Weckx and J. Driesen, "Load balancing with ev chargers and pv inverters in unbalanced distribution grids," *IEEE Transactions on Sustainable Energy*, vol. 6, no. 2, pp. 635–643, 2015.
[18] E. Dall'Anese, G. B. Giannakis, and B. F. Wollenberg, "Optimization of unbalanced power distribution networks via semidefinite relaxation," in *2012 North American Power Symposium (NAPS)*. IEEE, 2012, pp. 1–6.
[19] B. A. Robbins and A. D. Domínguez-García, "Optimal reactive power dispatch for voltage regulation in unbalanced distribution systems," *IEEE Transactions on Power Systems*, vol. 31, no. 4, pp. 2903–2913, 2015.
[20] L. R. Araujo, D. Penido, S. Carneiro, and J. L. R. Pereira, "A three-phase optimal power-flow algorithm to mitigate voltage unbalance," *IEEE Transactions on Power Delivery*, vol. 28, no. 4, pp. 2394–2402, 2013.
[21] X. Su, M. A. Masoum, and P. J. Wolfs, "Optimal pv inverter reactive power control and real power curtailment to improve performance of unbalanced four-wire lv distribution networks," *IEEE Transactions on Sustainable Energy*, vol. 5, no. 3, pp. 967–977, 2014.
[22] Q. Nguyen, H. V. Padullaparti, K.-W. Lao, S. Santoso, X. Ke, and N. Samaan, "Exact optimal power dispatch in unbalanced distribution systems with high pv penetration," *IEEE Transactions on Power Systems*, vol. 34, no. 1, pp. 718–728, 2018.
[23] K. Sheshyekani, I. Jendoubi, M. Teymuri, M. Hamzeh, H. Karimi, and M. Bayat, "Participation of distributed resources and responsive loads to voltage unbalance compensation in islanded microgrids," *IET Generation, Transmission & Distribution*, vol. 13, no. 6, pp. 858–867, 2019.
[24] M. E. Baran and F. F. Wu, "Network reconfiguration in distribution systems for loss reduction and load balancing," *IEEE Power Engineering Review*, vol. 9, no. 4, pp. 101–102, 1989.
[25] H. Yuan, F. Li, Y. Wei, and J. Zhu, "Novel linearized power flow and linearized opf models for active distribution networks with application in distribution lmp," *IEEE Transactions on Smart Grid*, vol. 9, no. 1, pp. 438–448, 2016.
[26] T. Akbari and M. T. Bina, "Linear approximated formulation of ac optimal power flow using binary discretisation," *IET Generation, Transmission & Distribution*, vol. 10, no. 5, pp. 1117–1123, 2016.
[27] J. Smith, G. Hensley, and L. Ray, "Ieee recommended practice for monitoring electric power quality. revis," 2009.
[28] R. D. Zimmerman, C. E. Murillo-Sánchez, and R. J. Thomas, "Matpower: Steady-state operations, planning, and analysis tools for power systems research and education," *IEEE Transactions on power systems*, vol. 26, no. 1, pp. 12–19, 2010.
[29] K. Schneider, P. Phanivong, and J.-S. Lacroix, "Ieee 342-node low voltage networked test system," in *2014 IEEE PES general meeting—conference & exposition*. IEEE, 2014, pp. 1–5.